BB/L001276/1, and BB/M001601/1 to M.R.B.; and BB/M002128/1 and BB/R001499/1 to J.M.C.). **Author contributions:** M.P., J.P., J.M.C., and M.R.B. designed the study; J.P. generated constructs, screened and isolated the *Arabidopsis* transgenic lines, and performed transient expression in tobacco; Y.W. carried out transient transformations and measurements in roots; M.P. performed the physiological and electrophysiological characterization of transgenic lines with assistance from L.H.; M.P., J.M.C., and M.R.B. analyzed the data; M.P., J.M.C., and M.R.B. wrote the manuscript. All authors discussed and commented on the manuscript. **Competing interests:** The authors declare no competing interests. **Data and materials availability:** Requests for materials should be addressed to M.R.B. and J.M.C. Stable BLINK1 transgenic lines of *Arabidopsis* in the wt and *p1p2* backgrounds are available under a material agreement with Plant Bioscience Ltd., Norwich, and the University of Glasgow. All of the data pertaining to the work are contained within the figures and supplementary materials.

SUPPLEMENTARY MATERIALS

www.sciencemag.org/content/363/6434/1456/suppl/DC1
Material and Methods
Figs. S1 to S8
Tables S1 to S3
References (*30*–*40*)

9 November 2018; accepted 27 February 2019
10.1126/science.aaw0046

WILDLIFE DISEASE

Amphibian fungal panzootic causes catastrophic and ongoing loss of biodiversity

Ben C. Scheele[1,2,3]*, Frank Pasmans[4], Lee F. Skerratt[3], Lee Berger[3], An Martel[4], Wouter Beukema[4], Aldemar A. Acevedo[5,6], Patricia A. Burrowes[7], Tamilie Carvalho[8], Alessandro Catenazzi[9], Ignacio De la Riva[10], Matthew C. Fisher[11], Sandra V. Flechas[12,13], Claire N. Foster[1], Patricia Frías-Álvarez[3], Trenton W. J. Garner[14,15], Brian Gratwicke[16], Juan M. Guayasamin[17,18,19], Mareike Hirschfeld[20], Jonathan E. Kolby[3,21,22], Tiffany A. Kosch[3,23], Enrique La Marca[24], David B. Lindenmayer[1,2], Karen R. Lips[25], Ana V. Longo[26], Raúl Maneyro[27], Cait A. McDonald[28], Joseph Mendelson III[29,30], Pablo Palacios-Rodriguez[12], Gabriela Parra-Olea[31], Corinne L. Richards-Zawacki[32], Mark-Oliver Rödel[20], Sean M. Rovito[33], Claudio Soto-Azat[34], Luís Felipe Toledo[8], Jamie Voyles[35], Ché Weldon[15], Steven M. Whitfield[36,37], Mark Wilkinson[38], Kelly R. Zamudio[28], Stefano Canessa[4]

Anthropogenic trade and development have broken down dispersal barriers, facilitating the spread of diseases that threaten Earth's biodiversity. We present a global, quantitative assessment of the amphibian chytridiomycosis panzootic, one of the most impactful examples of disease spread, and demonstrate its role in the decline of at least 501 amphibian species over the past half-century, including 90 presumed extinctions. The effects of chytridiomycosis have been greatest in large-bodied, range-restricted anurans in wet climates in the Americas and Australia. Declines peaked in the 1980s, and only 12% of declined species show signs of recovery, whereas 39% are experiencing ongoing decline. There is risk of further chytridiomycosis outbreaks in new areas. The chytridiomycosis panzootic represents the greatest recorded loss of biodiversity attributable to a disease.

Highly virulent wildlife diseases are contributing to Earth's sixth mass extinction (*1*). One of these is chytridiomycosis, which has caused mass amphibian die-offs worldwide (*2*, *3*). Chytridiomycosis is caused by two fungal species, *Batrachochytrium dendrobatidis* [discovered in 1998, (*4*)] and *B. salamandrivorans* [discovered in 2013, (*5*)]. Both *Batrachochytrium* species likely originated in Asia, and their recent spread has been facilitated by humans (*5*, *6*). Twenty years after the discovery of chytridiomycosis, substantial research has yielded insights about its epidemiology (*2*, *3*, *7*, *8*), yet major knowledge gaps remain. First, the global extent of species declines associated with chytridiomycosis is unknown [see (*2*, *9*) for initial assessments]. Second, although some regional declines are well studied, global spatial and temporal patterns of chytridiomycosis impacts remain poorly quantified. Third, ecological and life history traits have been examined only for a portion of declined species (*10*, *11*). Finally, after initial declines, it is unknown what proportion of declined species exhibit recovery, stabilize at lower abundance, or continue to decline. Here we present a global epidemiological analysis of the spatial and temporal extent of amphibian biodiversity loss caused by chytridiomycosis.

We conducted a comprehensive examination of evidence from multiple sources, including the International Union for Conservation of Nature (IUCN) Red List of Threatened Species (*12*), peer-reviewed literature, and consultation with amphibian experts worldwide (data S1). We classified declined species into five decline-severity categories corresponding to reductions in abundance. Species declines were attributed to chytridiomycosis on the basis of diagnosis of infection causing mortalities in the wild or, if this was unavailable, evidence consistent with key epidemiological characteristics of this disease. Most evidence is retrospective because many species declined before the discovery of chytridiomycosis (data S1).

We conservatively report that chytridiomycosis has contributed to the decline of at least 501 amphibian species (6.5% of described amphibian species; Figs. 1 and 2). This represents the greatest documented loss of biodiversity attributable to a pathogen and places *B. dendrobatidis* among the most destructive invasive species, comparable to rodents (threatening 420 species) and cats (*Felis catus*) (threatening 430 species) (*13*). Losses associated with chytridiomycosis are orders of magnitude greater than for other high-profile wildlife pathogens, such as white-nose syndrome (*Pseudogymnoascus destructans*) in bats (six species) (*14*) or West Nile virus (*Flavivirus* sp.) in birds (23 species) (*15*). Of the 501 declined amphibian species, 90 (18%) are confirmed or presumed extinct in the wild, with a further 124 (25%) experiencing a >90% reduction in abundance (Figs. 1 and 2). The declines of all species except one (*Salamandra salamandra* affected by *B. salamandrivorans*) were attributed to *B. dendrobatidis*.

Declines were proportional to taxonomic abundance, with anurans having 93% of severe declines (they comprise 89% of all amphibian species). Within anurans, there has been marked taxonomic clustering of declines, with 45% of severe declines and extinctions occurring in the Neotropical genera *Atelopus*, *Craugastor*, and *Telmatobius* (Fig. 2) (*16*). Chytridiomycosis is lethal to caecilians (*17*), but there have been no caecilian declines due to the disease, although data are limited. The capacity for *B. dendrobatidis* to cause major declines is attributable to its maintenance of high pathogenicity (*2*, *18*), broad host range (*8*), high transmission rate within and among host species (*2*, *7*), and persistence in reservoir host species and the environment (*19*). For many species, chytridiomycosis is the principal driver of decline, exemplified by precipitous mass mortalities in undisturbed environments (*2*). In other species, chytridiomycosis acts in concert with habitat loss, altered climatic conditions, and invasive species to exacerbate species declines (*20*).

Most amphibian declines have occurred in the tropics of Australia, Mesoamerica, and South America (Fig. 1), supporting the hypothesis that *B. dendrobatidis* spread from Asia into the New World (*6*). Asia, Africa, Europe, and North America have had notably low numbers of declines attributable to chytridiomycosis, despite widespread occurrence of *B. dendrobatidis* (*8*). Relative lack of documented declines could reflect less knowledge

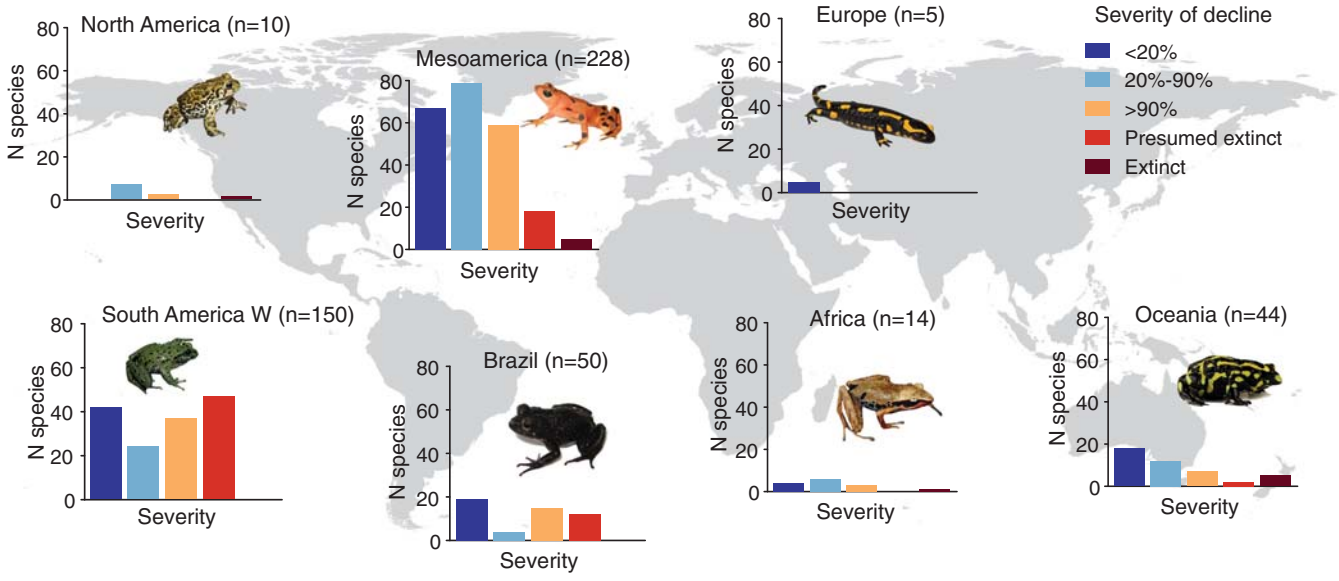

Fig. 1. Global distribution of chytridiomycosis-associated amphibian species declines. Bar plots indicate the number (N) of declined species, grouped by continental area and classified by decline severity. Brazilian species are plotted separately from all other South American species (South America W); Mesoamerica includes Central America, Mexico, and the Caribbean Islands; and Oceania includes Australia and New Zealand. No declines have been reported in Asia. *n*, total number of declines by region. [Photo credits (clockwise from top left): *Anaxyrus boreas*, C. Brown, U.S. Geological Survey; *Atelopus varius*, B.G.; *Salamandra salamandra*, D. Descouens, Wikimedia Commons; *Telmatobius sanborni*, I.D.I.R; *Cycloramphus boraceiensis*, L.F.T.; *Cardioglossa melanogaster*, M.H.; and *Pseudophryne corroboree*, C. Doughty]

[1]Fenner School of Environment and Society, Australian National University, Canberra, ACT 2601, Australia. [2]National Environmental Science Programme, Threatened Species Recovery Hub, Canberra, ACT 2601, Australia. [3]One Health Research Group, Melbourne Veterinary School, The University of Melbourne, Werribee, VIC 3030, Australia. [4]Wildlife Health Ghent, Department of Pathology, Bacteriology, and Avian Diseases, Faculty of Veterinary Medicine, Ghent University, B-9820 Merelbeke, Belgium. [5]Programa de Doctorado en Ciencias Biológicas, Laboratorio de Biología Evolutiva, Pontificia Universidad Católica de Chile, Avenida Libertador Bernardo O'Higgins 340, Santiago, Chile. [6]Grupo de Investigación en Ecología y Biogeografía, Universidad de Pamplona, Barrio El Buque, Km 1, Vía a Bucaramanga, Pamplona, Colombia. [7]Department of Biology, University of Puerto Rico, P.O. Box 23360, San Juan, Puerto Rico. [8]Laboratório de História Natural de Anfíbios Brasileiros (LaHNAB), Departamento de Biologia Animal, Instituto de Biologia, Universidade Estadual de Campinas, Campinas, Brazil. [9]Department of Biological Sciences, Florida International University, Miami, FL 33199, USA. [10]Museo Nacional de Ciencias Naturales-CSIC, C/ José Gutiérrez Abascal 2, Madrid 28006, Spain. [11]MRC Centre for Global Infectious Disease Analysis, School of Public Health, Imperial College London, London W2 1PG, UK. [12]Department of Biological Sciences, Universidad de los Andes, Bogotá, Colombia. [13]Instituto de Investigación de Recursos Biológicos Alexander von Humboldt, Sede Venado de Oro, Paseo Bolívar 16-20, Bogotá, Colombia. [14]Institute of Zoology, Zoological Society London, Regents Park, London NW1 4RY, UK. [15]Unit for Environmental Sciences and Management, North-West University, Potchefstroom 2520, South Africa. [16]Smithsonian National Zoological Park and Conservation Biology Institute, Washington, DC 20008, USA. [17]Universidad San Francisco de Quito USFQ, Colegio de Ciencias Biológicas y Ambientales COCIBA, Instituto de Investigaciones Biológicas y Ambientales BIOSFERA, Laboratorio de Biología Evolutiva, Campus Cumbayá, Quito, Ecuador. [18]Centro de Investigación de la Biodiversidad y Cambio Climático (BioCamb), Ingeniería en Biodiversidad y Cambio Climático, Facultad de Medio Ambiente, Universidad Tecnológica Indoamérica, Calle Machala y Sabanilla, Quito, Ecuador. [19]Department of Biology, Colorado State University, Fort Collins, CO 80523, USA. [20]Museum für Naturkunde, Leibniz Institute for Evolution and Biodiversity Science, Invalidenstr. 43, Berlin 10115, Germany. [21]Honduras Amphibian Rescue and Conservation Center, Lancetilla Botanical Garden and Research Center, Tela, Honduras. [22]The Conservation Agency, Jamestown, RI 02835, USA. [23]AL Rae Centre for Genetics and Breeding, Massey University, Palmerston North 4442, New Zealand. [24]School of Geography, Faculty of Forestry Engineering and Environmental Sciences, University of Los Andes, Merida, Venezuela. [25]Department of Biology, University of Maryland, College Park, MD 20742, USA. [26]Department of Biology, University of Florida, Gainesville, FL 32611, USA. [27]Laboratorio de Sistemática e Historia Natural de Vertebrados. Facultad de Ciencias, Universidad de la República. Igua 4225, CP 11400, Montevideo, Uruguay. [28]Department of Ecology and Evolutionary Biology, Cornell University, Ithaca, NY 14853, USA. [29]Zoo Atlanta, Atlanta, GA 30315, USA. [30]School of Biological Sciences, Georgia Institute of Technology, Atlanta, GA 30332, USA. [31]Departamento de Zoología, Instituto de Biología, Universidad Nacional Autónoma de México, Mexico City, México. [32]Department of Biological Sciences, University of Pittsburgh, Pittsburgh, PA 15260, USA. [33]Unidad de Genómica Avanzada (Langebio), Centro de Investigación y de Estudios Avanzados del Instituto Politécnico Nacional, km 9.6 Libramiento Norte Carretera Irapuato-León, Irapuato, Guanajuato CP36824, México. [34]Centro de Investigación para la Sustentabilidad, Facultad de Ciencias de la Vida, Universidad Andres Bello, Santiago 8370251, Chile. [35]Department of Biology, University of Nevada, Reno, NV 89557, USA. [36]Zoo Miami, Conservation and Research Department, Miami, FL 33177, USA. [37]Florida International University School of Earth, Environment, and Society, 11200 SW 8th St., Miami, FL 33199, USA. [38]Department of Life Sciences, The Natural History Museum, London SW7 5BD, UK.
***Corresponding author. Email: ben.scheele@anu.edu.au**

of amphibian populations in Asia and Africa (*3*, *21*), early introduction and potential coevolution of amphibians and *B. dendrobatidis* in parts of Africa and the Americas [e.g., (*22*)], the comparatively recent emergence of *B. dendrobatidis* in Western and Northeast Africa (*6*), or unsuitable conditions for chytridiomycosis. It remains unknown whether chytridiomycosis contributed to widespread amphibian declines reported in North America and Europe in the 1950s to 1960s (*3*, *21*, *22*) or current enigmatic salamander declines in eastern North America. Although the number of new declines has now eased (Fig. 3), additional declines could occur if *B. dendrobatidis* or *B. salamandrivorans* are introduced into new areas, highly virulent lineages are introduced into areas that currently have less-virulent lineages (*6*), and/or environmental changes alter previously stable pathogen-host dynamics (*3*).

Chytridiomycosis-associated declines peaked globally in the 1980s, between one and two decades before the discovery of the disease (Fig. 3 and table S1), and coincident with anecdotal recognition of amphibian declines in the 1990s (*23*). A second, smaller peak occurred in the early 2000s, associated with an increase in declines in western South America (Fig. 3 and fig. S1). Regionally, temporal patterns of decline are variable (fig. S1). For example, in some areas of South America and Australia, declines commenced in the late 1970s (*2*, *24*), whereas in other areas, declines started in the 2000s (*25*). *B. dendrobatidis* is associated with ongoing declines in 197 assessed species. Ongoing declines after a transition to enzootic disease dynamics (*19*) might be driven by a lack of effective host defenses, maintenance of high pathogenicity (*18*), and presence of *B. dendrobatidis* in amphibian and nonamphibian reservoirs (*7*, *19*).

We examined host life history traits and environmental conditions to understand why some species declined more severely than others, using multinomial logistic regression and accounting for the degree of evidence that chytridiomycosis was implicated in each species's decline (fig. S2

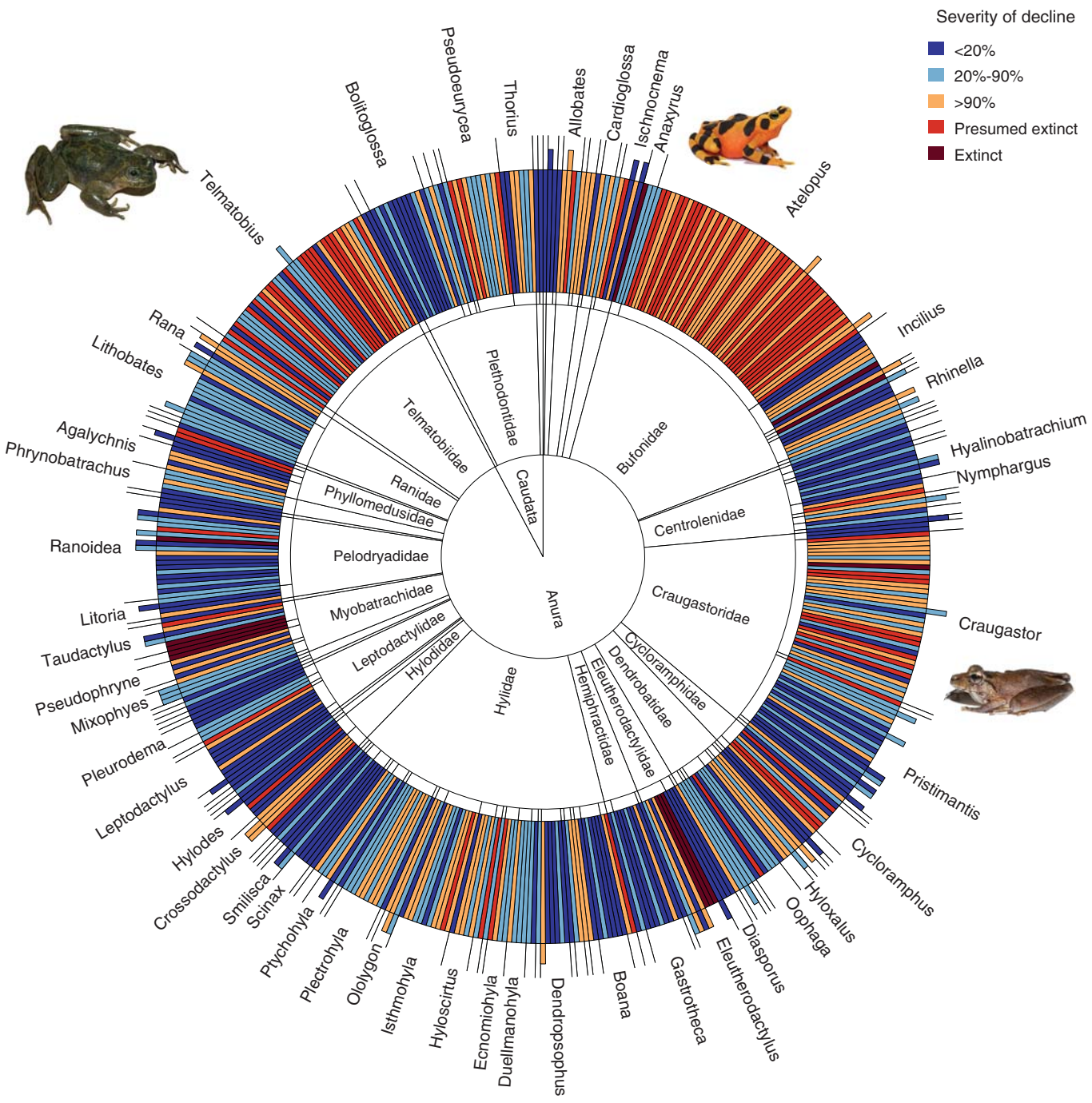

Fig. 2. Taxonomic distribution of chytridiomycosis-associated amphibian declines. Each bar represents one species, and color denotes the severity of its decline. Concentric circles indicate, from inner to outer, order (Caudata or Anura), family, and genus. Full names are given only for families and genera that include >5 and >2 species, respectively; details for all taxa are in table S4. Within each taxonomic level, sublevels are ordered alphabetically. Protruding bars indicate species for which there is evidence of recovery. [Photo credits (left to right): *Telmatobius bolivianus*, I.D.I.R.; *Atelopus zeteki*, B.G.; and *Craugastor crassidigitus*, B.G.]

and table S2). Decline severity was greatest for larger-bodied species, those occurring in consistently wet regions, and those strongly associated with perennial aquatic habitats. These patterns are likely due to favorable environmental conditions for *B. dendrobatidis* in wet regions (*7*), because the fungus dies when desiccated, as well as the general pattern of increased time to maturity in large-bodied amphibians resulting in less reproductive potential to offset mortality due to chytridiomycosis (*26*). Declines were less severe for species with large geographic and elevational ranges (Fig. 4), potentially owing to the greater chance of their range encompassing environmental conditions unfavorable for *B. dendrobatidis* (*3*) and/or information bias, because population extinctions can be assessed with more certainty in restricted-range species. Our results are consistent with previous studies that show that the risk of chytridiomycosis is associated with host aquatic habitat use, large body size, and narrow elevational range (*10*, *11*).

Encouragingly, of the 292 surviving species for which population trends are known, 60 (20%) have shown initial signs of recovery. However, recoveries generally represent small increases in abundance of individual populations, not

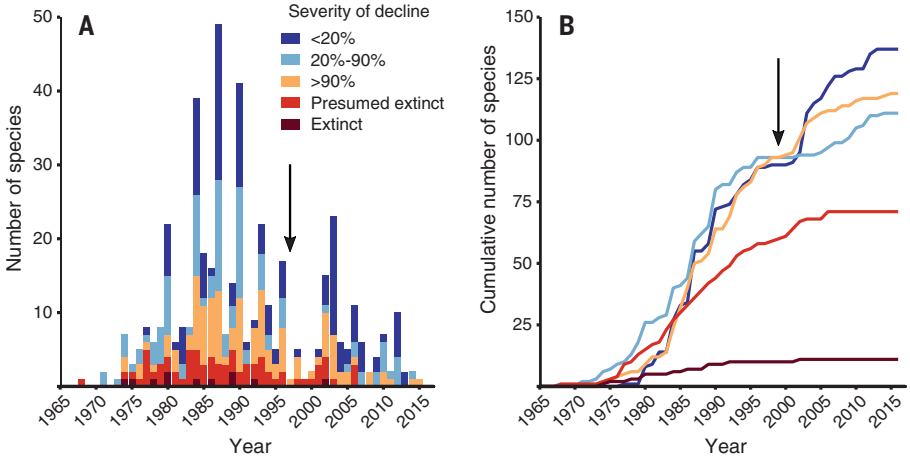

Fig. 3. Timing of chytridiomycosis-associated amphibian declines. (**A**) Declines by year. Bars indicate the number of declines in a given year, stacked by decline severity. For species for which the exact year of decline is uncertain, the figure shows the middle year of the interval of uncertainty, as stated by experts or inferred from available data. (**B**) Cumulative declines. Curves indicate the cumulative number of declines in each decline-severity category over time. In (A) and (B), the arrows mark the discovery of chytridiomycosis in 1998.

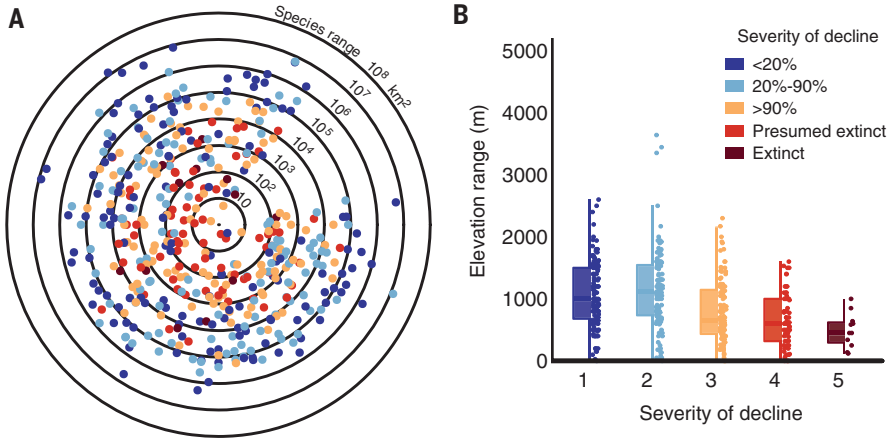

Fig. 4. Severity of chytridiomycosis-associated amphibian declines in relation to the geographic and elevational ranges of species. (**A**) Declines in relation to geographic range. Each dot indicates a species, located randomly along the perimeter of a circle with radius equal to the $\log_{10}$ of the species's geographic range in kilometers squared. (**B**) Declines in relation to elevational range. Horizontal bars, boxes, and vertical bars indicate, respectively, mean, first and second quartiles, and 95% quantiles of elevation ranges within each category of decline severity.

complete recovery at the species level. Logistic regression showed the probability of recovery was lower for species that experienced more recent or more severe declines, for large-bodied or nocturnal species, and for species occurring at higher elevations (fig. S2 and table S3). When holding those predictors of recovery at their mean value, the chance of a species recovering from a severe (>90%) decline was less than 1 in 10. Low probability of recovery for high-elevation species might be related to suitable climatic conditions for fungal persistence as well as limited connectivity to source populations and/or longer host generation time (*26*). Some recoveries may be underpinned by selection for increased host resistance (*18*), whereas management of concurrent threats may have facilitated other recoveries (a promising avenue for conservation interventions) (*27*). Unfortunately, the remaining 232 species have shown no signs of recovery.

The unprecedented lethality of a single disease affecting an entire vertebrate class highlights the threat from the spread of pathogens in a globalized world. Global trade has recreated a functional Pangaea for infectious diseases in wildlife, with far-reaching impacts on biodiversity (this study), livestock (*28*), and human health (*29*). Effective biosecurity and an immediate reduction in wildlife trade are urgently needed to reduce the risk of pathogen spread. As mitigation of chytridiomycosis in nature remains unproven (*30*), new research and intensive monitoring that utilizes emerging technologies are needed to identify mechanisms of species recovery and develop new mitigation actions for declining species.

REFERENCES AND NOTES

1. M. C. Fisher *et al.*, *Nature* **484**, 186–194 (2012).
2. L. F. Skerratt *et al.*, *EcoHealth* **4**, 125–134 (2007).
3. K. R. Lips, *Philos. Trans. R. Soc. Lond. B Biol. Sci.* **371**, 20150465 (2016).
4. L. Berger *et al.*, *Proc. Natl. Acad. Sci. U.S.A.* **95**, 9031–9036 (1998).
5. A. Martel *et al.*, *Science* **346**, 630–631 (2014).
6. S. J. O'Hanlon *et al.*, *Science* **360**, 621–627 (2018).
7. T. Y. James *et al.*, *Ecol. Evol.* **5**, 4079–4097 (2015).
8. D. H. Olson *et al.*, *PLOS ONE* **8**, e56802 (2013).
9. S. N. Stuart *et al.*, *Science* **306**, 1783–1786 (2004).
10. J. Bielby, N. Cooper, A. A. Cunningham, T. W. J. Garner, A. Purvis, *Conserv. Lett.* **1**, 82–90 (2008).
11. K. R. Lips, J. D. Reeve, L. R. Witters, *Conserv. Biol.* **17**, 1078–1088 (2003).
12. The IUCN Red List of Threatened Species, Version 2017-3 (IUCN Species Survival Commission, Gland, Switzerland); www.iucnredlist.org.
13. T. S. Doherty, A. S. Glen, D. G. Nimmo, E. G. Ritchie, C. R. Dickman, *Proc. Natl. Acad. Sci. U.S.A.* **113**, 11261–11265 (2016).
14. W. E. Thogmartin *et al.*, *Biol. Conserv.* **160**, 162–172 (2013).
15. T. L. George *et al.*, *Proc. Natl. Acad. Sci. U.S.A.* **112**, 14290–14294 (2015).
16. E. La Marca *et al.*, *Biotropica* **37**, 190–201 (2005).
17. D. J. Gower *et al.*, *EcoHealth* **10**, 173–183 (2013).
18. J. Voyles *et al.*, *Science* **359**, 1517–1519 (2018).
19. A. Valenzuela-Sánchez *et al.*, *Proc. Biol. Sci.* **284**, 20171176 (2017).
20. D. B. Wake, V. T. Vredenburg, *Proc. Natl. Acad. Sci. U.S.A.* **105** (suppl. 1), 11466–11473 (2008).
21. J. E. Houlahan, C. S. Findlay, B. R. Schmidt, A. H. Meyer, S. L. Kuzmin, *Nature* **404**, 752–755 (2000).
22. B. L. Talley, C. R. Muletz, V. T. Vredenburg, R. C. Fleischer, K. R. Lips, *Biol. Conserv.* **182**, 254–261 (2015).
23. D. B. Wake, *Science* **253**, 860–860 (1991).
24. K. R. Lips, J. Diffendorfer, J. R. Mendelson III, M. W. Sears, *PLOS Biol.* **6**, e72 (2008).
25. A. Catenazzi, E. Lehr, L. O. Rodriguez, V. T. Vredenburg, *Conserv. Biol.* **25**, 382–391 (2011).
26. C. Morrison, J. M. Hero, *J. Anim. Ecol.* **72**, 270–279 (2003).
27. R. A. Knapp *et al.*, *Proc. Natl. Acad. Sci. U.S.A.* **113**, 11889–11894 (2016).
28. A. K. Wiethoelter, D. Beltrán-Alcrudo, R. Kock, S. M. Mor, *Proc. Natl. Acad. Sci. U.S.A.* **112**, 9662–9667 (2015).
29. K. J. Olival *et al.*, *Nature* **546**, 646–650 (2017).
30. T. W. Garner *et al.*, *Philos. Trans. R. Soc. Lond. B Biol. Sci.* **371**, 20160207 (2016).

ACKNOWLEDGMENTS

We thank M. Arellano, E. Courtois, A. Cunningham, K. Murray, S. Ron, R. Puschendorf, J. Rowley, and V. Vredenburg for discussions on amphibian declines. Comments from two anonymous reviewers greatly improved the manuscript.
Funding: B.C.S. and D.B.L. were supported by the Australian National Environmental Science Program. L.B., L.F.S., T.A.K., and B.C.S. were supported by the Australian Research Council (grants FT100100375, LP110200240, and DP120100811), the NSW Office of Environment and Heritage, and the Taronga Conservation Science Initiative. S.C., W.B., A.M., and F.P. were supported by Research Foundation Flanders grants FWO3E001916 and FWO11ZK916N-11ZK918N and Ghent University grant BOF16/GOA/024. S.C. was supported by Research Foundation Flanders grant FWO16/PDO/019. A.A.A. was supported by the Conservation Leadership Program (0621310), Vicerrectoría de Investigaciones, Universidad de Pamplona-Colombia, and Colciencias (1121-659-44242). T.C. was supported by the Coordination for the Improvement of Higher Education Personnel. A.C. was supported by the Amazon Conservation Association, the Amphibian Specialist Group, the Disney Worldwide Conservation Fund, the Eppley Foundation, the Mohammed bin Zayed Species Conservation Fund, the NSF, the Rufford Small Grants Foundation, and the Swiss National Foundation. I.D.l.R. was supported by the Spanish Government (CGL2014-56160-P). M.C.F. was supported by the NERC (NE/K014455/1), the Leverhulme Trust (RPG-2014-273), and the Morris Animal Foundation (D16ZO-022). S.V.F. was supported by the USFWS Wildlife without Borders (96200-0-G228), the AZA–Conservation Endowment Fund (08-836), and the Conservation International Critically Endangered Species Fund. P.F.Á. was supported by a Postdoctoral Research fellowship

from the Mexican Research Council (CONACYT, 171465). T.W.J.G. was supported by the NERC (NE/N009967/1 and NE/K012509/1). J.M.G. was supported by the Universidad San Francisco de Quito (collaboration grants 11164 and 5447). M.H. was supported by scholarships from the Elsa-Neumann-Foundation and the German Academic Exchange Service (DAAD). C.A.M. was supported by the Atkinson Center for a Sustainable Future and the Cornell Center for Vertebrate Genomics. G.P.-O. was supported by DGAPA-UNAM and CONACYT while on sabbatical at the University of Otago, New Zealand. C.L.R.-Z. was supported by the NSF (1660311). S.M.R. was supported by a CONACYT Problemas Nacionales grant (PDCPN 2015-721) and a UC Mexus-Conacy cooperative grant.

C.S.-A. was supported by the Chilean National Science and Technology Fund (Fondecyt no. 1181758). L.F.T. was supported by the São Paulo Research Foundation (FAPESP 2016/25358-3) and the National Council for Scientific and Technological Development (CNPq 300896/2016-6). J.V. was supported by the NSF (DEB-1551488 and IOS-1603808). C.W. was supported by the South African National Research Foundation. **Author contributions:** B.C.S., F.P., L.B., L.F.S., A.M., and S.C. conceived the research. B.C.S. collated the data and coordinated data collection. All authors contributed ideas and data. S.C. conducted the analysis, with input from B.C.S., F.P., A.M., C.N.F., and W.B. B.C.S., F.P., L.B., L.F.S., A.M., C.N.F., and S.C. wrote the paper with input from all authors. **Competing interests:** The authors declare no competing interests. **Data and materials availability:** All data are available in the manuscript or the supplementary materials.

SUPPLEMENTARY MATERIALS

www.sciencemag.org/content/363/6434/1459/suppl/DC1
Materials and Methods
Figs. S1 and S2
Tables S1 to S4
References (*31*–*47*)
Data S1

9 August 2018; accepted 6 February 2019
10.1126/science.aav0379

RNA SEQUENCING

Slide-seq: A scalable technology for measuring genome-wide expression at high spatial resolution

Samuel G. Rodriques[1,2,3]*, Robert R. Stickels[3,4,5]*, Aleksandrina Goeva[3], Carly A. Martin[3], Evan Murray[3], Charles R. Vanderburg[3], Joshua Welch[3], Linlin M. Chen[3], Fei Chen[3]†‡, Evan Z. Macosko[3,6]†‡

Spatial positions of cells in tissues strongly influence function, yet a high-throughput, genome-wide readout of gene expression with cellular resolution is lacking. We developed Slide-seq, a method for transferring RNA from tissue sections onto a surface covered in DNA-barcoded beads with known positions, allowing the locations of the RNA to be inferred by sequencing. Using Slide-seq, we localized cell types identified by single-cell RNA sequencing datasets within the cerebellum and hippocampus, characterized spatial gene expression patterns in the Purkinje layer of mouse cerebellum, and defined the temporal evolution of cell type–specific responses in a mouse model of traumatic brain injury. These studies highlight how Slide-seq provides a scalable method for obtaining spatially resolved gene expression data at resolutions comparable to the sizes of individual cells.

The functions of complex tissues are fundamentally tied to the organization of their resident cell types. Multiplexed in situ hybridization and sequencing-based approaches can measure gene expression with subcellular spatial resolution (*1*–*3*) but require specialized knowledge and equipment, as well as the upfront selection of gene sets for measurement. By contrast, technologies for spatially encoded RNA sequencing with barcoded oligonucleotide capture arrays are limited to resolutions in hundreds of micrometers (*4*), which are insufficient to detect important tissue features.

To develop our Slide-seq technology for high-resolution genome-wide expression analysis, we first packed uniquely DNA-barcoded 10-μm microparticles ("beads")—similar to those used in the Drop-seq approach for single-cell RNA sequencing (scRNA-seq) (*5*)—onto a rubber-coated glass coverslip to form a monolayer we termed a "puck" (fig. S1). We found that each bead's distinct barcode sequence could be determined via SOLiD (sequencing by oligonucleotide ligation and detection) chemistry (Fig. 1A and fig. S1) (*6*–*8*). We next developed a protocol wherein 10-μm fresh-frozen tissue sections were transferred onto the dried bead surface via cryosectioning (*7*). mRNA released from the tissue was captured onto the beads for preparation of 3′-end, barcoded RNA-seq libraries (*5*) (Fig. 1B). Clustering of individual bead profiles from a coronal section of mouse hippocampus (*7*) yielded assignments reflecting known positions of cell types in the tissue (Fig. 1C). Very fine spatial features were resolved, including the single-cell ependymal cell layer between the central ventricle and the habenula in the mouse brain (Fig. 1C, inset). Moreover, Slide-seq could be applied to a range of tissues, including the cerebellum and olfactory bulb, where layered tissue architectures were immediately detectable (Fig. 1D and fig. S2), as well as the liver and kidney, where the identified clusters revealed hepatocyte zonation patterns (*9*) and the cellular constituents of the nephron, respectively. Slide-seq on postmortem human cerebellum was also successful in capturing the same architectural features observed in the cognate mouse tissue (fig. S3). Expression measurements by Slide-seq agreed with those from bulk mRNA-seq and scRNA-seq, and average mRNA transcript capture per cell was consistent across tissues and experiments (fig. S4). Finally, we found no detectable difference in the dimensions of brain structures analyzed by Slide-seq and fluorescence in situ hybridization (fig. S5), implying that mRNA is transferred from the tissue to the beads with minimal lateral diffusion.

To map scRNA-seq cell types onto Slide-seq data, we developed a computational approach called non-negative matrix factorization regression (NMFreg) that reconstructs expression of each Slide-seq bead as a weighted combination of cell type signatures defined by scRNA-seq (Fig. 2A). Application of NMFreg to a coronal mouse cerebellar puck recapitulated the spatial distributions of classical neuronal and non-neuronal cell types (*10*), such as granule cells, Golgi interneurons, unipolar brush cells, Purkinje cells, and oligodendrocytes (Fig. 2B and fig. S6A). The mapping by NMFreg was found to be reliable across a range of factor numbers and random restarts (fig. S6, B and C). We found that 65.8 ± 1.4% of beads could be matched with a single cell type (*7*), whereas 32.6 ± 1.2% showed mRNA from two cell types (mean ± SD, $N = 7$ cerebellar pucks) (Fig. 2C and fig. S7). The high spatial resolution of Slide-seq was key to mapping cell types: When data were aggregated into larger feature sizes, cell types in heterogeneous regions of tissue could not be resolved (fig. S8). Slide-seq collects a two-dimensional (2D) spatial sample of 3D tissue volumes, and thus caution should be taken when making absolute counting measurements throughout the 3D volume in the absence of proper stereological controls and sampling methods (*11*).

We first sequenced pucks capturing 66 sagittal tissue sections from a single dorsal mouse hippocampus, covering a volume of 9 mm^3, with ~10-μm resolution in the dorsal-ventral and anterior-posterior axes and ~20-μm resolution (alternate 10-μm sections) in the medial-lateral axis (fig. S9, A to D). 1.5 million beads, of which 770,000 could be associated with a single scRNA-seq–defined cell type using NMFreg, were mapped to short-read sequencing data in the volume. We computationally co-registered pucks along the medial-lateral axis, allowing for visualization of the cell types

[1]Department of Physics, Massachusetts Institute of Technology, Cambridge, MA 02139, USA. [2]MIT Media Lab, Massachusetts Institute of Technology, Cambridge, MA 02139, USA. [3]Broad Institute of Harvard and MIT, Cambridge, MA 02142, USA. [4]Graduate School of Arts and Sciences, Harvard University, Cambridge, MA 02138, USA. [5]Division of Medical Science, Harvard Medical School, Boston, MA 02115, USA. [6]Department of Psychiatry, Massachusetts General Hospital, Boston, MA 02114, USA.
*These authors contributed equally to this work.
†These authors contributed equally to this work.
‡Corresponding author. Email: chenf@broadinstitute.org (F.C.); emacosko@broadinstitute.org (E.Z.M.)